"Brick and Mortar" Strategy for the Formation of Highly Crystalline Mesoporous Titania Films from Nanocrystalline Building Blocks

Johann M. Szeifert,[‡,†] Dina Fattakhova-Rohlfing,[‡,†] Dimitra Georgiadou,[†] Vit Kalousek,[§] Jiri Rathouský,[§] Daibin Kuang,[||] Sophie Wenger,[||] Shaik M. Zakeeruddin,[||] Michael Grätzel,[||] and Thomas Bein*[,†]

Department of Chemistry and Biochemistry and Center for NanoScience (CeNS), University of Munich (LMU), Germany, J. Heyrovský Institute of Physical Chemistry, Academy of Sciences of the Czech Republic, and Laboratory of Photonics and Interfaces, Institute of Chemical Sciences and Engineering, Ecole Polytechnique Fédérale de Lausanne, Switzerland

Received October 26, 2008. Revised Manuscript Received December 16, 2008

We present a novel "brick and mortar" strategy for creating highly efficient transparent TiO_2 coatings for photocatalytic and photovoltaic applications. Our approach is based on the fusion of preformed titania nanocrystalline "bricks" through surfactant-templated sol−gel titania "mortar", which acts as a structure-directing matrix and as a chemical glue. The similar chemical composition of both bricks and mortar leads to a striking synergy in the interaction of crystalline and amorphous components, such that crystallization is enhanced upon thermal treatment and highly porous and highly crystalline structures are formed at very mild conditions. Coatings with a broad variety of periodic mesostructures and thicknesses ranging from few nanometers to several micrometers are accessible using the same organic template, and the final structures are tunable by varying the fraction of the "bricks". The beneficial combination of crystallinity and porosity leads to greatly enhanced activity of the films in photocatalytic processes, such as the photooxidation of NO. Acting as the active layers in dye-sensitized solar cells, films of only 2.7 μm in thickness exhibit a conversion efficiency of 6.0%.

Introduction

Nanostructured films of TiO_2 have an enormous potential for applications in photocatalysis, solar cells, sensors, and energy storage.[1] However, reaching this potential often requires films that simultaneously feature both large and easily accessible surface area and highly crystalline pore walls. Crystalline titania layers are most commonly assembled from crystalline particles by sintering.[2,3] This approach offers very good control over the phase composition and the degree of crystallinity, but lacks the possibility to tune the structure and the porosity. To overcome these shortcomings, researchers employ molecular/oligomeric precursors (sols) in a templated sol−gel process.[4−7] Thus, precise control over the porosity by using structure directing agents[8−11] can be achieved, but the crystallinity of the resulting TiO_2 frameworks is usually only moderate and high calcination temperatures are needed for further crystallization.[12,13] Here we present a novel preparation strategy that not only combines the strong points of both above-mentioned techniques, but also extends the material's functionality by introducing further control over physical properties beyond the scope of the classical techniques. This is achieved by the fusion of preformed titania nanocrystals with surfactant-templated sol−gel titania, which acts as a structure-directing matrix and as a chemical glue.[14] This technique can be described as a "brick and mortar" approach, a term which has been introduced for the preparation of composite materials.[15−18] The uniqueness of our approach consists in the similar chemical composition of both the "bricks" and the "mortar", such that the latter acts as a reactive precursor

* Corresponding author. Fax: 49 89 2180 77622. E-mail: bein@lmu.de.
† University of Munich.
‡ These authors contributed equally to this work.
§ Academy of Sciences of the Czech Republic.
|| Ecole Polytechnique Fédérale de Lausanne.

(1) Linsebigler, A. L.; Lu, G.; Yates, J. T. *Chem. Rev.* **1995**, *95*, 735–758.
(2) O'Regan, B.; Gratzel, M. *Nature* **1991**, *353*, 737–740.
(3) Kavan, L.; Gratzel, M.; Rathousky, J.; Zukal, A. *J. Electrochem. Soc.* **1996**, *143*, 394–400.
(4) Choi, S. Y.; Lee, B.; Carew, D. B.; Mamak, M.; Peiris, F. C.; Speakman, S.; Chopra, N.; Ozin, G. A. *Adv. Funct. Mater.* **2006**, *16*, 1731–1738.
(5) Choi, S. Y.; Mamak, M.; Coombs, N.; Chopra, N.; Ozin, G. A. *Adv. Funct. Mater.* **2004**, *14*, 335–344.
(6) Crepaldi, E. L.; Soler-Illia, G.; Grosso, D.; Cagnol, F.; Ribot, F.; Sanchez, C. *J. Am. Chem. Soc.* **2003**, *125*, 9770–9786.
(7) Sanchez, C.; Boissiere, C.; Grosso, D.; Laberty, C.; Nicole, L. *Chem. Mater.* **2008**, *20*, 682–737.
(8) Brinker, C. J.; Lu, Y. F.; Sellinger, A.; Fan, H. Y. *Adv. Mater.* **1999**, *11*, 579–585.
(9) Yang, P. D.; Zhao, D. Y.; Margolese, D. I.; Chmelka, B. F.; Stucky, G. D. *Chem. Mater.* **1999**, *11*, 2813–2826.
(10) Grosso, D.; Boissiere, C.; Smarsly, B.; Brezesinski, T.; Pinna, N.; Albouy, P. A.; Amenitsch, H.; Antonietti, M.; Sanchez, C. *Nat. Mater.* **2004**, *3*, 787–792.
(11) Sel, O.; Kuang, D. B.; Thommes, M.; Smarsly, B. *Langmuir* **2006**, *22*, 2311–2322.
(12) Carreon, M. A.; Choi, S. Y.; Mamak, M.; Chopra, N.; Ozin, G. A. *J. Mater. Chem.* **2007**, *17*, 82–89.
(13) Choi, S. Y.; Mamak, M.; Speakman, S.; Chopra, N.; Ozin, G. A. *Small* **2005**, *1*, 226–232.
(14) Stathatos, E.; Chen, Y.; Dionysiou, D. D. *Solar Energy Mater. Solar Cells* **2008**, *92*, 1358–1365.

10.1021/cm8029246 CCC: $40.75
Published on Web 03/23/2009

Scheme 1. Formation of Crystalline Mesoporous Titania Films (right side) via the "Brick and Mortar" Approach; Nanocrystalline Titania "Bricks" (light blue, left side) are Dispersed in Amorphous Titania "Mortar" (grey), Which Is Periodically Self-Assembled around the Micelles of the Polymer Template (magenta)

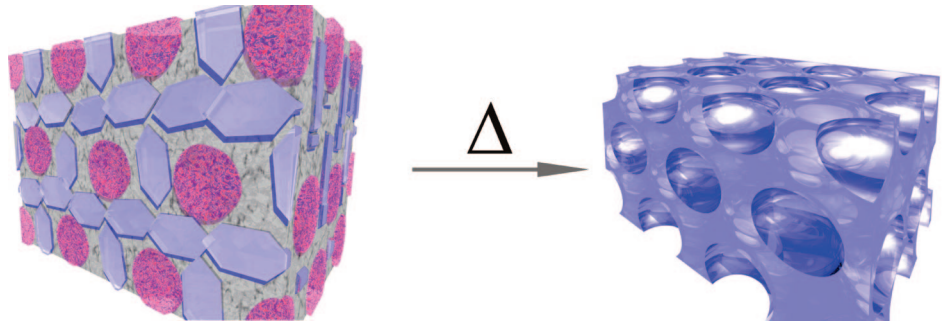

for the further growth of the crystalline phase seeded by the nanocrystals. This synergy leads to a drastically lowered temperature needed for crystallization (Scheme 1). Moreover, the films exhibit high transparency, tunable thickness over a wide range from tens of nanometers to several micrometers, and strong adhesion to the substrate.

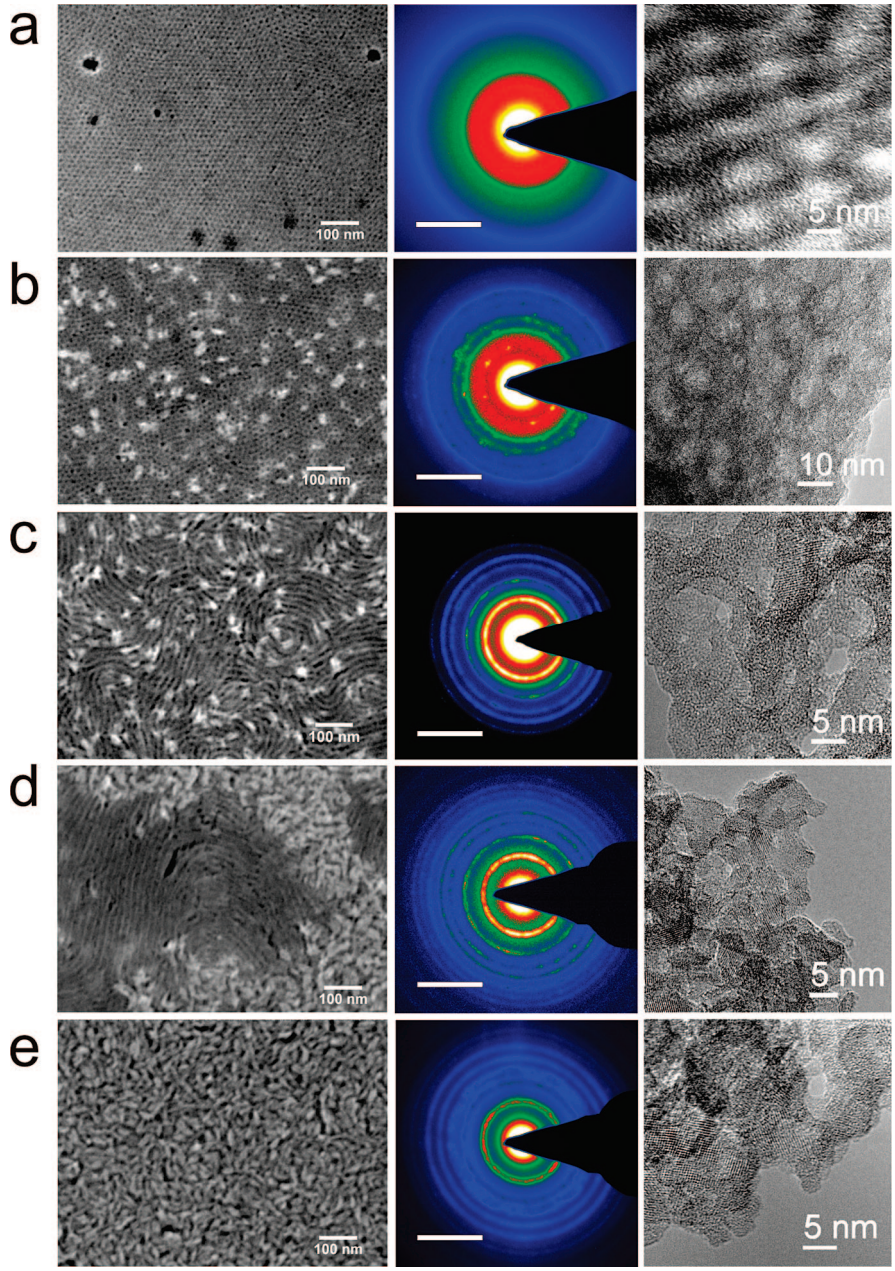

Figure 1. SEM images on silicon substrate (first column), HRTEM images (third column), and the corresponding SAED patterns (second column) of the composite titania films containing (a) 0, (b) 10, (c) 15, (d) 30, and (e) 100% of titania nanoparticles.

Table 1. Texture Data of Mesoporous Titania Films

percentage of nanoparticles (%)	S_{BET}[a] (m^2/g)	S_{BET}[b] (cm^2/cm^2)	V_{TOT}[c] (cm^3/g)	V_{TOT}[d] (mm^3/cm^2)	D (nm)
0	89	118	0.132	0.010	3−4[e]
10		98		0.0086	3−4[e]
15	71	110	0.180	0.0107	7.5
30	52	77	0.210	0.013	6−7
50	62	57	0.325	0.0142	10
100		68		—[f]	—[f]

[a] From adsorption isotherms of toluene at 25 °C, using the cross-sectional area of toluene of 0.314 nm^2 calculated from the density of the liquid adsorptive in the bulk liquid state. [b] From adsorption isotherms of krypton at 77 K, using the cross-sectional area of krypton of 0.210 nm^2. The BET surface area was related to the geometrical area of the support. [c] From adsorption isotherms of toluene at 25 °C, using the molar volume of liquid toluene. [d] From adsorption isotherms of krypton at 77 K, using the molar volume of solid krypton. The volume was related to the geometrical area of the support. [e] Average value for a bimodal texture (wider cavities with narrow necks). [f] Isotherm of a macroporous material. Pore size and volume are not determinable from Kr sorption experiments. D = pore diameter.

Results and Discussion

The synthesis of the titania nanocrystalline "bricks" was inspired by a nonaqueous route originally developed by M. Niederberger at al.[19,20] Completely crystalline particles of 4−5 nm in size are formed by the reaction of titanium tetrachloride with benzyl alcohol at low temperatures (see Figure S1 in the Supporting Information). We found that the resulting particles redisperse easily in tetrahydrofuran (THF) at high concentrations exceeding 5 wt % in the presence of the Pluronic 123 block-copolymer (PEO_{20}-PPO_{70}-PEO_{20}). The latter promotes stabilization of the particles and acts as a structure directing agent in the film assembly. The sol of titania "mortar" was prepared by the hydrolysis of tetraethyl orthotitanate catalyzed by hydrochloric acid.[21] For the preparation of the nanocomposite films, the "mortar" was added to the colloidal solution of "bricks" at ratios ranging from 0 to 100 wt % (related to the total mass of TiO_2 formed after calcination). The dip-coated titania films were calcined at 300 °C in order to induce further crystal growth and to remove the copolymer.

The results of transmission electron microscopy (TEM), small-angle X-ray scattering (SAXS, see Figure S2 in the Supporting Information), scanning electron microscopy (SEM) images, and physical sorption experiments clearly show that the introduction of crystalline titania nanoparticles into surfactant-templated titania precursor sols has a dramatic influence on the porous structure and crystallinity of the calcined films. Although the pure sol−gel derived amorphous films exhibit a well-defined 3D-cubic arrangement of mesopores 7 nm in size with a periodicity of 14 nm (Figure 1a), deterioration of the mesostructure occurs upon addition of small amounts of particles, accompanied by some increase in the crystallinity (Figure 1b). When the fraction of the titania nanoparticles exceeds a critical value of 15 wt %, a channeled, fingerprintlike structure is formed with greatly increased crystallinity (Figure 1c). A further increase in the concentration of nanoparticles leads to a phase separation and coexistence of a channeled structure and domains of a particulate phase having a different mesoporous structure (Figure 1d). The latter phase becomes dominant when the particle fraction exceeds 50%.

Addition of different amounts of titania nanoparticles also changes the character of porosity (Table 1 and Figure 2). In pure sol−gel films, the spherical pores are connected with each other via openings of the ink-bottle type[22] with restricted accessibility. Addition of titania nanoparticles at ≥15 wt % induces an increase in pore size and pore volume and an opening of the pore system. Higher concentrations of anatase particles lead to the creation of roughly cylindrical mesopores with a substantially increased size and the complete removal of pore blocking.

The crystallinity of the films prepared by the "brick and mortar" approach was found to increase dramatically upon calcination at the relatively low temperature of only 300 °C. This development of crystallinity was demonstrated by quantitative X-ray diffraction using a crystalline standard as a reference and comparing the (101) anatase peak integral (Figure 3). As the crystallinity increases much faster than the percentage of added crystalline particles, the crystalline building blocks must have induced the crystallization of the surrounding sol−gel matrix and acted as seeds for the crystallization of amorphous titania. Above a percentage of approximately 50%, the crystallinity reaches a plateau that corresponds to the maximum value of crystallinity.

The titania films prepared by the "brick and mortar" approach were investigated in some of their most important applications, namely in photocatalysis and in dye-sensitized solar cells (DSC).

The photooxidation of NO was selected as a suitable photocatalytic reaction because of its environmental importance.[25] Low concentrations of nitrogen oxides remaining in the atmosphere after the burning of fuels present a major environmental risk in cities. Highly crystalline mesoporous films of TiO_2 are especially suitable for the removal of NO because of their large surface area, as the heterogeneous photodecomposition processes are dependent on the amount of surface-adsorbed reactants. The studied films can be roughly divided into three groups according to their photoactivity (Figure 4a). The films with a nanoparticle content of 50−70% are the most active ones, the stationary (steady state) photoconversion reaching about 9%. Those prepared without nanocrystals are much less active; the stationary conversion is only about 4%. Interestingly, the films prepared exclusively from nanocrystals without any sol−gel "mortar"

(15) Boal, A. K.; Ilhan, F.; DeRouchey, J. E.; Thurn-Albrecht, T.; Russell, T. P.; Rotello, V. M. *Nature* **2000**, *404*, 746–748.
(16) Arumugam, P.; Xu, H.; Srivastava, S.; Rotello, V. M. *Polym. Int.* **2007**, *56*, 461–466.
(17) Liu, R.; Ren, Y.; Shi, Y.; Zhang, F.; Zhang, L.; Tu, B.; Zhao, D. *Chem. Mater.* **2008**, *20*, 1140–1146.
(18) Peng, T. Y.; Zhao, D.; Dai, K.; Shi, W.; Hirao, K. *J. Phys. Chem. B* **2005**, *109*, 4947–4952.
(19) Niederberger, M.; Bartl, M. H.; Stucky, G. D. *Chem. Mater.* **2002**, *14*, 4364–4370.
(20) Niederberger, M.; Garnweitner, G.; Pinna, N.; Neri, G. *Prog. Solid State Chem.* **2005**, *33*, 59–70.
(21) Alberius, P. C. A.; Frindell, K. L.; Hayward, R. C.; Kramer, E. J.; Stucky, G. D.; Chmelka, B. F. *Chem. Mater.* **2002**, *14*, 3284–3294.
(22) Ravikovitch, P. I.; Vishnyakov, A.; Neimark, A. V.; Carrott, M.; Russo, P. A.; Carrott, P. J. *Langmuir* **2006**, *22*, 513–516.
(23) Klug, H. P. A., L. E. *X-Ray Diffraction Procedures*; John Wiley & Sons: New York, 1974; p 716.
(24) Laskowski, J. J.; Young, J.; Gray, R.; Acheson, R.; Forder, S. D. *Anal. Chim. Acta* **1994**, *286*, 9–23.

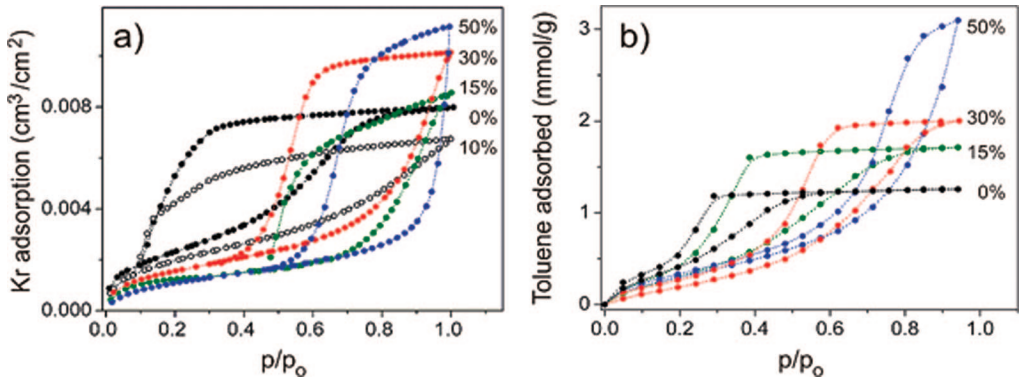

Figure 2. Adsorption isotherms of (a) krypton at 77 K and (b) toluene at 298 K on "brick and mortar" titania films calcined at 300 °C. The labels indicate the particle content in the initial solution.

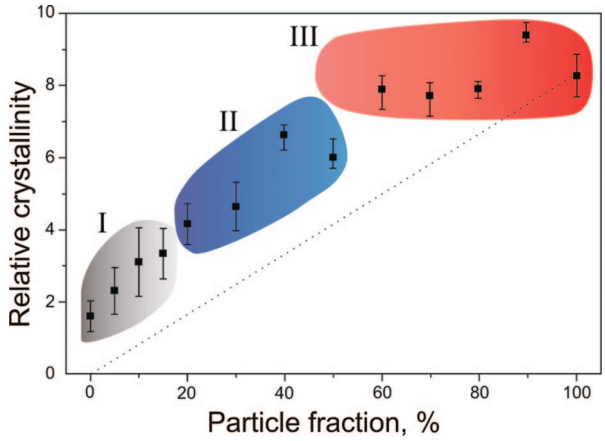

Figure 3. Diagram showing the development of crystallinity in samples from cast solutions after calcination at 300 °C as a function of the fraction of nanoparticles in the precursor solution. The data points (average of 3 experiments) were calculated using the internal standard method (see Experimental Section).[23,24] In short, the integral of (101) anatase was divided by that of the standard (111) fluorite, and normalized to the value of the sample that contains 100% crystalline particles; the error bars indicate the standard deviation. This is correlated to the formation of different mesoporous structures as observed by electron microscopy and sorption methods: distorted cubic mesophase (I), channeled structure (II), and particulate phase (III). The dotted line shows the theoretical crystallinity of the films before calcination.

addition also exhibit low conversion efficiency, most probably due to the lower surface area and less favorable pore structure. Thus, the "brick and mortar" layers are very promising materials for photocatalytic applications because of their high efficiency in the degradation of NO. The additional advantages of "brick and mortar" layers in this context are high transparency (see Figure S5 in the Supporting Information) and excellent optical qualities in combination with strong adhesion to the substrate. This makes them attractive candidates for large-area coatings on glass panels and windows in buildings, where mechanical stability and transparency are essential.

A similar nonlinear change in performance was also observed for photovoltaic cells fabricated from films with different particle content (panels c and d in Figure 4 and Table S1 in the Supporting Information). The films prepared from a sol−gel precursor without particles exhibit very low photocurrent and conversion efficiency. The performance increases more than 7-fold when 15 wt% of nanocrystals are added to the initial solution, and still improves with a further increase in particle content. This effect, similar to that observed for the photocatalytic performance, clearly reflects the drastic changes in the degree of crystallinity of the titania material. It is supported also by the photocurrent transient studies (see Figure S3 in the Supporting Information), which indicate electron collection problems due to the insufficient crystallinity of titania layers containing less than 30% particles. We note that TiO_2 films prepared from 100% nanoparticles exhibit much worse photovoltaic efficiency in spite of their complete crystallinity, the former being about 45% lower than the values for the films containing 30% nanocrystals. The mild calcination temperature of 300 °C is apparently not sufficient for sintering the particles via solid-state diffusion. In contrast, the fast viscous sintering of the amorphous sol−gel (mortar) component followed by its crystallization enables efficient fusion of the particles and provides the necessary electrical contact. The binding role of the sol−gel component also becomes evident in the obvious difference in the mechanical stability of the nanocomposite films. While the 100% particulate films are rather fragile and easily scratched off the substrate, films containing the sol−gel precursor are much more robust and mechanically stable.

Films with widely varying thickness can be prepared by the "brick and mortar" approach. The coating procedure can be repeated several times leading to a linear increase in thickness, surface area and pore volume without any significant change in the nature of the porosity. This feature is drastically different from the classical sol−gel templated films. For the latter, the surface area and pore volume can be increased at maximum by 4−5 times compared to a single coating, whereas further coating/calcination cycles lead to a degradation of the porous system.[27,28]

As expected, the photovoltaic efficiency is improved after increasing the thickness of the titania layer. The optimum

(25) Galloway, J. N.; Townsend, A. R.; Erisman, J. W.; Bekunda, M.; Cai, Z.; Freney, J. R.; Martinelli, L. A.; Seitzinger, S. P.; Sutton, M. A. *Science* **2008**, *320*, 889–892.

(26) Kuang, D. B.; Klein, C.; Ito, S.; Moser, J. E.; Humphry-Baker, R.; Evans, N.; Duriaux, F.; Graetzel, C.; Zakeeruddin, S. M.; Graetzel, M. *Adv. Mater.* **2007**, *19*, 1133–1137.

(27) Zukalova, M.; Prochazka, J.; Zukal, A.; Yum, J. H.; Kavan, L. *Inorg. Chim. Acta* **2008**, *361*, 656–662.

(28) Prochazka, J.; Kavan, L.; Shklover, V.; Zukalova, M.; Frank, O.; Kalbac, M.; Zukal, A.; Pelouchova, H.; Janda, P.; Week, K.; Klementova, M.; Carbone, D. *Chem. Mater.* **2008**, *20*, 2985–2993.

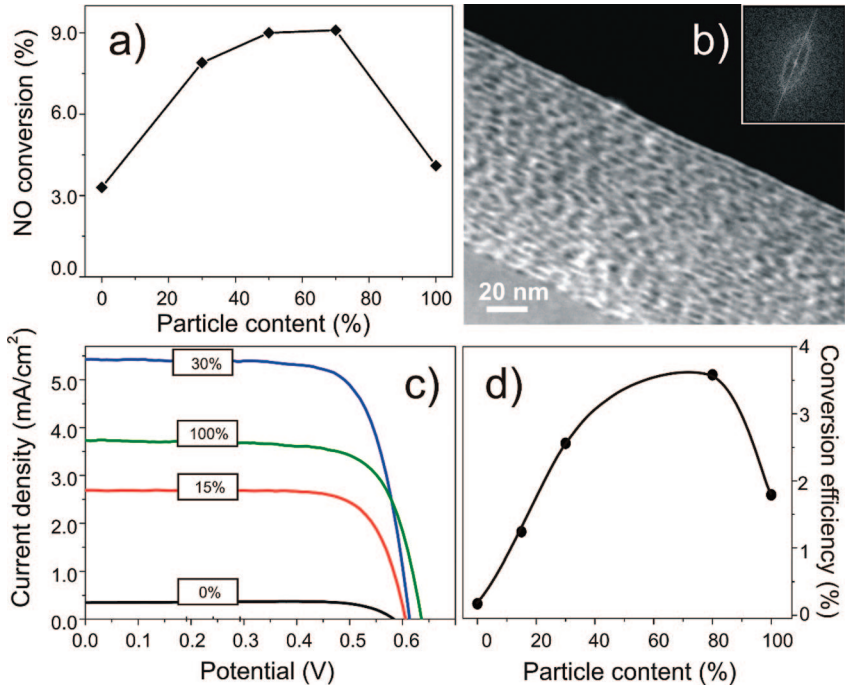

Figure 4. Photocatalytic degradation of NO on titania films with different particle content: (a) steady-state conversion efficiency and (b) cross-sectional STEM-HAADF image of one of the highly photoactive films containing 50% of titania particles. Inset: Fourier transform of the picture revealing the regular pore shape. (c) Photocurrent−voltage curve and (d) dependence of conversion efficiency of DSC devices based on the "brick and mortar" titania layers with a nanoparticle content ranging from 0 to 100 wt %, D205 sensitizer, and Z646 electrolyte.[26] The titania layer thickness was ca. 1.0 μm. The photovoltaic performance was measured at air mass 1.5 (100 mW/cm^2) full sunlight illumination. The active cell area was 0.158 cm^2.

performance was found for films prepared using 80 wt % anatase nanoparticles. The cell based on such a film with 2.7 μm in thickness gives, under standard global AM 1.5 full sunlight (100 mW/cm^2) illumination, a short circuit photocurrent density (J_{sc}) of 10.7 mA/cm^2, an open circuit potential (V_{oc}) of 745 mV, and a fill factor (FF) of 0.75, yielding a total conversion efficiency of 6.0% (see Figure S4 in the Supporting Information). This is impressively high for such thin films in combination with a nonvolatile electrolyte and makes them serious candidates for photoanodes in dye-sensitized solar cells.

In conclusion, the "brick and mortar" approach for the formation of mesoporous crystalline materials shows a striking synergy in the interactions of crystalline and amorphous components. The distinctive feature of this approach is the ability to create highly porous and highly crystalline structures at very mild conditions. A broad variety of mesostructures is accessible using the same organic template, and the final structures are tunable by varying the fraction of the "bricks". This attractive strategy offers new opportunities for the design of nanostructured materials with enhanced functionality through various architectures with large accessible porosity and high crystallinity.

Experimental Section

Titanium dioxide nanoparticles were synthesized following a modified procedure by Niederberger et al.[19] Titanium tetrachloride (1.5 mL, 13.7 mmol) was dissolved in toluene (10 mL) and added to benzyl alcohol (30 mL, 291 mmol) under continuous stirring. The solution was kept at 60 °C for 20 h, then cooled down to room temperature. The particles were separated by centrifugation at 50000 rcf for 30 min and used without further treatment. As such, the particles contain about 55 wt % benzyl alcohol according to thermogravimetric analysis; this was taken into account for the adjustment of the TiO_2 content.

In a typical synthesis, a solution of Pluronic P123 (0.2 g, 0.04 mmol) in THF (4 mL) was added to nonwashed particles (0.2 g, 1.1 mmol of TiO_2, previously separated by centrifugation) and stirred overnight until the particles were homogeneously redispersed. Subsequently, the desired amount of sol−gel (SG, see below) solution (for example, 0.9 mL, with 2.51 mmol of TiO_2, for the solution containing 30% particles) was added, followed by stirring for several minutes. The final solutions were transparent or translucent, and yellow to orange in color. The SG solution was prepared by adding hydrochloric acid (37%, 5.1 mL, 62.1 mmol) to tetraethyl orthotitanate (7.2 mL, 34.3 mmol) at room temperature under continuous stirring.

The mass ratio of nanoparticles to the sol−gel precursor was varied, but the total amount of TiO_2 was kept at 0.4 g (5.01 mmol). The Pluronic P123 content in the dip-coating solution was 50 wt % with respect to the total mass of TiO_2. As an example, the amount of TiO_2 in the solution containing 50% particles was 8.1 wt %. The films were prepared by dip-coating at 23 ± 2 °C and a relative humidity of 45 ± 10% at a withdrawal rate of 1.8 mm/s, and calcined at 300 °C (with a ramp of 0.6 °C min^{-1}) for 30 min.

Scanning electron microscopy (SEM) was performed on a JEOL JSM-6500F scanning electron microscope equipped with a field emission gun, at 4 kV. High-resolution transmission electron microscopy (HRTEM) and scanning transmission electron microscopy in high-angle annular dark-field mode (STEM-HAADF) was performed using a FEI Titan 80−300 equipped with a field-emission gun operated at 300 kV. The particulate samples were prepared by evaporating a drop of a diluted solution of particles with small amounts of Pluronic P123 in THF on a Plano holey carbon-coated copper grid. HRTEM of films was carried out by scraping the thin-film samples off the substrate onto a holey carbon-coated copper grid. The film thickness was measured by profilometry (Dektak),

ellipsometry using a Woolam ESM-300, and SEM. The porosity of the films was determined by the analysis of adsorption isotherms of Kr at the boiling point of liquid nitrogen (approximately 77 K) using an ASAP 2010 apparatus (Micromeritics). The toluene adsorption was carried out using a self-built Quartz Crystal Microbalance (QCM) system. For this purpose, the precursor solutions were spin-coated (3000 rpm, 30 s) on KVG 10 MHz QCM devices with gold electrodes (from Quartz Crystal Technology GmbH) and calcined at 300 °C. Toluene was used as an adsorptive and the measurements were performed at 25 °C. Raman spectra were recorded with a LabRAM HR UV−vis (Horiba Jobin Yvon) Raman microscope (Olympus BX41) with a Symphony CCD detection system using a HeNe laser at 632.8 nm. The spectra were taken from material removed from the substrate. X-ray diffraction analysis was carried out in reflection mode using a Scintag XDS 2000 (Scintag Inc.) with Ni-filtered Cu Kα-radiation.

The quantitative crystallinity measurements were performed using the internal standard method with fluorite, CaF_2, as internal standard.[23,24] For this purpose, the dip-coating solutions were cast into a wide calcination vessel, dried overnight at 60 °C, and calcined at 300 °C (with a ramp of 0.6 °C min^{-1}) for 30 min. The resulting film or powder was ground and thoroughly mixed with 10 wt% of fluorite. X-ray diffraction patterns were recorded using a STOE STADI P COMBI diffractometer. The diffraction peaks of (101) anatase and (111) fluorite were fitted with a Gaussian peak shape and integrated. The integral of (101) anatase was divided by that of (111) fluorite. This crystallinity value was normalized to that of the 100% particles sample, which after calcination is considered to be completely crystalline. The data points correspond to an average of three samples. The error bars indicate the standard deviation from the average.

The experimental setup for the photocatalytic tests consisted of a gas supply part, the photoreactor, and a chemiluminiscent $NO-NO_x$ gas analyzer (Horiba ambient monitor APNA-360). The gaseous reaction mixture was prepared by mixing streams of dry air (1500 mL/min), wet air (1500 mL/min, relative humidity of 100%), and 50 ppm NO/N_2 (approximately 60 mL/min), in order to obtain a final concentration of NO of 1 ppm at a relative humidity of 50%. The photoreactor was illuminated by four 8 W black lights, thus achieving a UV light intensity of 1 mW/cm^2. Prior to the photocatalytic tests, the photoreactor was purged with the NO/water vapor/air mixture without illumination until a steady NO concentration was achieved at the outlet. 100% NO conversion is equivalent to a photonic efficiency of $\xi = 0.14\%$ assuming a mean irradiation wavelength of 350 nm. The photonic efficiency was calculated on the basis of all the incoming light of the intensity of 1 mW/cm^2.

For photovoltaic measurements, the mesoporous TiO_2 films on FTO-coated glass substrates were heated at 200 °C for 30 min, cooled to ca. 80 °C, immersed into the dye solution at room temperature, and kept there for 16 h. The dye solution containing 0.3 mM indoline dye D205 (molar extinction coefficient of 53000 at 532 nm) in acetonitrile and *tert*-butyl alcohol (volume ratio 1:1) was used to sensitize the photoanode.[29] Dye-coated mesoporous TiO_2 films were assembled and sealed with a thin transparent hot-melt 25 μm thick Surlyn ring (DuPont) to the counter electrodes (Pt on FTO glass, chemical deposition from 0.005 M hexachloroplatinic acid in isopropanol, heated at 400 °C for 15 min). The electrolyte was injected into the inner electrode space from the counter electrode side through a predrilled hole, and the hole was then sealed with a Bynel sheet and a thin glass cover slide by heating. The nonvolatile electrolyte (Z646) contains 1.0 M PMII (propylmethylimidazolium iodide), 0.15 M iodine, 0.1 M GuNCS (guanidinium thiocyanate), and 0.5 M N-butyl benzimidazole (NBB) in 3-methoxypropionitrile.[26] The device assembly, the characterization of current density−voltage and incident photon to current conversion efficiency (IPCE) of the DSCs are described in detail elsewhere.[26]

Acknowledgment. This work was supported by the Nanosystems Initiative Munich (NIM) funded by the DFG in Germany. The authors thank Dr. Steffen Schmidt and Dr. Markus Döblinger for SEM and TEM measurements and Andreas Zürner for graphics design. We thank Prof. S. Uchida for the gift of the D205 dye and for developing and preparing this dye in collaboration with Dr. M. Takata, Dr. H. Miura, and Dr. K. Sumioka. J.R. and V.K. are thankful to the Grant Agency of the Czech Republic for the financial support (Grant 104/08/0435-1).

Supporting Information Available: TEM, XRD, and Raman spectra of titania particles and photovoltaic measurement data of films (PDF). This material is available free of charge via the Internet at http://pubs.acs.org.

CM8029246

(29) Kuang, D. B.; Wang, P.; Ito, S.; Zakeeruddin, S. M.; Gratzel, M. *J. Am. Chem. Soc.* **2006**, *128*, 7732–7733.